Proceedings of the CONF-MLA 2026 Symposium: Explainable Computing, Modeling & Data Science in Complex Systems
DOI: 10.54254/2755-2721/2026.GF36881

A Review of Deep Learning-Based Image Deblurring

Yuxuan Wu

International School, Beijing University of Posts and Telecommunications, Beijing, China
2025213687@bupt.cn

Abstract. As an urgent problem in image restoration, deblurring aims to recover the original clear image of a blurred picture that has been damaged by motion, defocus, etc. Most of the above are explicit blur-kernel estimates. However, the distribution of these is not uniform. With the progress of deep learning in recent years, many end-to-end methods have been developed based on CNNs, RNNs, GANs and Transformers to reduce the need for hand-crafted priors. The first is to list some types of blur and their corresponding formulas. Then, it will introduce the general ideas, typical examples and applications of the four main architectural styles, as well as their particular advantages and deficiencies in different blurring conditions. List some representative benchmark datasets and image quality assessment methods from the survey, then discuss the main problems of computational efficiency, cross-domain generalization and lightweight deployment, and future research directions.

Keywords: Image deblurring, deep learning, convolutional neural networks, generative adversarial networks, Transformer

1. Introduction

One kind of degradation is that the image is not sharp and some fine details have been lost during acquisition or transmission. Therefore, it can affect the performance of various vision tasks in surveillance and other applications. Generally, the four types of blur are classified according to their physical causes as motion blur, defocus blur, Gaussian blur and mixed blur. The first is the problem of recovering sharp images from blurred observations. Generally speaking, the degradation process of spatially invariant blur can be represented as the convolution of a latent sharp image and a blur kernel. The former is to solve deblurring as an inverse deconvolution problem [1]. Camera shake, object motion and changes in scene depth will all cause a spatially varying blur of the image. Therefore, the performance of the former method is quite poor. Many of the optimisation measures are too complicated to be implemented in actual production. Recently, deep learning [2, 3] has been able to realise the entire mapping from a blurry observation to a clear picture. These methods avoid explicit blur-kernel estimation. They can automatically extract multiscale hierarchical features and handle complex, spatially nonuniform degradations. Existing approaches mainly include CNN-, RNN-, GAN-, and Transformer-based methods. These methods show differences in feature extraction, local–global dependency modeling, and optimization strategies.

© 2026 The Authors. This is an open access article distributed under the terms of the Creative Commons Attribution License 4.0 (https://creativecommons.org/licenses/by/4.0/).

DOI: 10.54254/2755-2721/2026.GF36881

This survey systematically reviews deep-learning-based image deblurring methods. It summarizes the physical causes and formulations of representative blur types. The discussion covers CNN-, RNN-, GAN-, and Transformer-based approaches, focusing on their characteristics and limitations. Benchmark datasets plus image-quality assessment criteria are also introduced for evaluation.

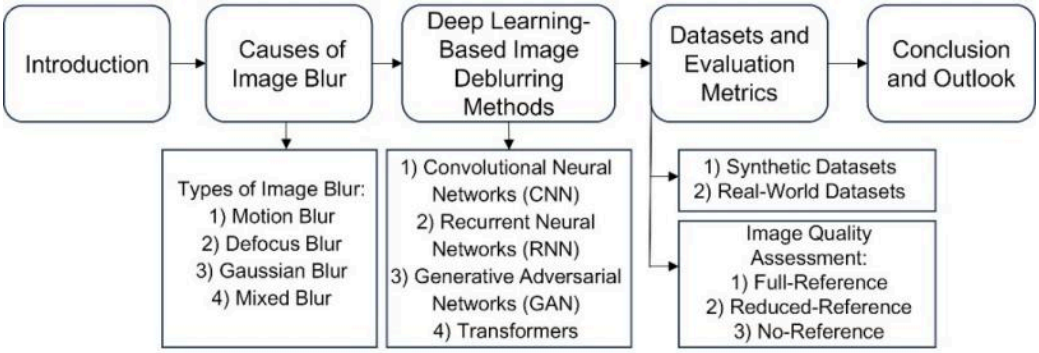

Figure 1. Organization and scope of this survey

2. Causes of image blur

2.1. Problem formulation

Image blur may result from motion, defocus, Gaussian degradation, or a combination of multiple factors. A general image degradation model can be expressed as [4]: $B = \emptyset\left(I_s, k\right) + N$, where φ denotes the image degradation operator, B is the observed blurred image, I_s is the latent sharp image, k is the blur kernel, and N represents additive noise. Image deblurring aims to recover the latent sharp image by approximating the inverse of the degradation process, expressed as follows $I_{db} = \emptyset^{-1}\left(B, k, N\right)$, where φ^{-1} denotes the deblurring model and I_{db} is the restored sharp image.

2.2. Motion blur

Motion blur usually occurs when the camera and/or subject is moving during the interval of exposure. Early studies tended to assume that the blur kernel was the same across all the spatial locations and modelled the degradation as a convolution process. The classical methods used image edges, textures and gradients to define blur and to reconstruct sharp structures. These methods estimated a spatially uniform blur kernel, and recovered image details using translation-invariance constraints, gradient priors, and total-variation regularization based on the physical imaging model [5].

2.3. Defocus blur

Defocus blur is when the scene is not on the camera focal plane and it becomes blurred. The light rays from a point source will not focus accurately at the focus. This point source is subsequently captured as a spot which is bigger than the point, called the circle of confusion. Conditions that have an effect on perceived sharpness include magnification, imaging distance and viewing distance. A circle of confusion that is less than the visual resolution threshold is normally not noticeable. This threshold sets the maximum amount of allowed circle of confusion. The difference between the two permissible circles of confusion, one before and one after the focal plane, is the depth of field.

DOI: 10.54254/2755-2721/2026.GF36881

Objects outside this region are affected by defocus blur and this is usually modeled by a point-spread function [6].

2.4. Gaussian blur

The Gaussian blur is a convolution of an image with a Gaussian kernel. The two dimensional Gaussian kernel is defined as: $G(x,y) = \frac{1}{2\pi\sigma^2} e^{-\frac{x^2+y^2}{2\sigma^2}}$. Here σ is the standard deviation of the Gaussian kernel which determines the amount of blurring. The greater the value of σ, the more smoothing will be done. $G(x,y)$ denotes the kernel value at spatial location (x,y).

2.5. Mixed blur

Blur in real world imaging can be caused by camera shake, object motion and scene-depth variation. This is because complex degradation makes it hard to accurately estimate the blur-kernel. Most of the recent research has used CNNs and other deep learning models to directly learn representations of blurs from data. However, strong motion deblurring, accurate kernel estimation and restoration in the presence of compound degradation is still an open task. Another important aspect of effective methods is that they must also be able to balance the process of removing blur and preserving fine textures and structural details.

3. Deep learning-based image deblurring

Deep-learning-based image deblurring has received extensive attention in computer vision. Unlike conventional approaches, deep models can directly restore a sharp image from a blurred input without explicitly estimating the blur magnitude or kernel. This section reviews four representative methodological families: CNNs [5, 7], RNNs [3, 8], GANs [9, 10], and Transformers [11, 12].

3.1. CNN-based methods

CNN-based deblurring methods use stacked convolution and pooling operations to learn features of blurred images or blur kernels and reconstruct sharp outputs. Sun et al. [5] were among the first to introduce CNNs into image deblurring, predicting the probability distribution of patch-level motion kernels. Gong et al. [7] have used contextual image information to train a fully convolutional network that can approximate a dense motion-flow representation of the blur kernel. Xu et al. [13] used CNNs to detect and correct the main features in the image based on edge prediction, then inferred the blur kernel. Ren et al. [14] used Maximum A Posteriori (MAP) estimation with deep models and an asymmetric autoencoder having skip connections to obtain the latent sharp image, and then a fully connected network was used to generate the blur kernel. Fang et al. [15] have put forward a latent-prior-based method for nonuniform kernel estimation, and a normalizing-flow model is used to map motion blur kernels into a Gaussian latent representation and then predict the kernels in this learned feature space.

The above methods can reconstruct fine details in the image. A CNN can learn the relationship between the blurred input and the corresponding sharp image directly, so there will be no error in kernel estimation. Nah et al. [2] have built a general CNN framework to reconstruct sharp images from blurry observations, and Dong et al. [16] have made full use of the multiscale redundancy in natural images to construct a CNN-based denoiser for blur removal. Process the image at various

DOI: 10.54254/2755-2721/2026.GF36881

scales to keep the structure and details. Zhang et al. [17] have put forward a multi-scale loss function and a spatial pyramid structure to gradually introduce fine details from coarse to fine. Cho et al. [18] have changed the traditional coarse-to-fine strategy and introduced MIMO-UNet, a multi-input multi-output U-Net that can perform deblurring at different scales.

Although CNNs are effective, they have only local convolutional operations and thus lack the ability to consider the whole picture and long-term relationships. There will be artifacts or structural deformation in the event of severe motion blur. Expanding the Receptive Field usually increases the computation; thus, pixel-wise reconstruction loss may over-smooth the output and lose fine details.

3.2. RNN-based methods

RNNs handle the problem of sequence dependence. Recurrent operations are employed in blind image deblurring to pass hidden states from the previously processed region or scale to the current step, and thus the network can learn correlations among local features and gradually reduce blur. Zhang et al. [3] have employed the spatial variation of RNNs to implicitly model the deblurring process, and recurrent computation has been carried out in both space and time to restore the structure and texture of the image. Tao et al. [8] have put forward a scale-recurrent deblurring network with shared weights at different scales to reduce the training difficulty. Hidden-state propagation has information at all scales and gradually retrieves it. Therefore, Gao et al. [19] have put forward parameter-selective sharing and nested skip connections to better deal with the scale-dependent characteristics of images.

Park et al. [20] need to learn too many parameters for multi-scale feature extraction; thus, they have adopted a multi-temporal method. Divide the image into several blurred regions and process them one by one at the original resolution to reduce the model size. Zhang et al. [21] later put forward a two-stage hybrid network for the actual motion deblurring. The first is a recurrent encoder-decoder that produces recurrent features, and in the second stage, these features are used with the blurred image to gradually reconstruct it. RNNs are good at capturing context, but they are inherently sequential and therefore not easily parallelised; as a result, they are slower to train and run. Errors at the start of the recurrent steps will be accumulated and carried over, affecting the stability and accuracy of the final reconstruction.

3.3. GAN-based methods

The two parts of a GAN are a generator and a discriminator; both are trained in an adversarial manner. The generator of image deblurring is trained to convert a blurred input into a clear reconstruction, and the discriminator determines whether the restored image is in the distribution of clear images. Kupyn et al. [9] employed residual blocks in the generator and a PatchGAN discriminator in DeblurGAN. Adversarial optimisation will probably have the problem of vanishing or exploding gradients. DeblurGAN-v2 [10] is a feature-pyramid generator and a relativistic discriminator. The Discriminator learns to weigh the importance of global and local features differently. Lu et al. [22] employed dual-content and blur encoders, and then introduced adversarial and cycle-consistency losses to regularise the generation process. Zhang et al. [23] have combined a blur-generation GAN with a deblurring GAN to reduce the domain difference between synthetic and real-world blur. Yang et al. [24] have taken the features of shallow and deep networks to build latent-space mappings and noise representations, and then reconstructed both the general shape and local details. Li et al. [25] have added a blur-kernel discriminator to find errors in the estimated kernel and do not directly reconstruct a sharp image end-to-end. GAN training still has problems of

DOI: 10.54254/2755-2721/2026.GF36881

mode collapse and gradient instability, etc. Also, the adversarial objective is not in line with the distortion-oriented metrics of PSNR and SSIM. Therefore, the image may be perceived as reasonable but have a low objective score.

3.4. Transformer-based methods

Transformers have recently been applied to the problem of image deblurring. Vaswani and others first introduced Transformers in 2017 for sequence models in natural language processing, and later the Vision Transformer [11] was developed for images. The good performance of the above two is due to the combination of token-mixing operations [12] and feed-forward networks [26], and self-attention can be used to handle long-term dependencies well. However, the size of global self-attention grows exponentially with the number of tokens, and it is not practical to apply it directly to high-resolution images. To reduce the cost, the images are usually divided into non-overlapping patches and encoded as token sequences, and many efficient token mixers have been developed. Swin Transformer [27] has a hierarchical shifted-window attention to gradually gather features, and the Neighborhood Attention Transformer restricts attention to a small neighbourhood. Sparse Attention [28] and Hybrid Local-Global Attention Mechanisms [29] have also been introduced. Linformer [30] reduces the complexity by low-rank projection, and Linear Transformer [31] and Performer [12] approximate attention in a kernelised way. Although the designs above can improve the scalability of high-resolution restoration, if the model capacity and training conditions are relatively low, the performance increase will generally not be substantial; therefore, the whole architecture, optimisation and data Design should also be taken into account.

4. Datasets and evaluation metrics

4.1. Datasets

Existing image deblurring datasets are generally categorized into two types: synthetic datasets and real-world datasets. Synthetic datasets are generated using predefined blur processes [32]. They usually provide paired blurred and sharp images for supervised training and evaluation. Real-world datasets contain naturally blurred observations captured under practical conditions, such as camera shake, handheld imaging, and object motion [33]. These datasets better represent the degradation in real applications.

4.1.1. Synthetic datasets

The first synthetic benchmarks are the convolutions of sharp images with a fixed blur kernel. Levin et al. [32] have convolved the four sharp images with eight spatially invariant kernels to obtain 32 blurred images, but fixed resolution and a small number of scenes limit the range of this benchmark. Sun et al. [34] made 640 blurred pictures by convolving the 80 natural pictures with eight uniform kernels. Both datasets assume spatially invariant blur and are therefore not suitable for evaluating strongly nonuniform degradation. Köhler et al. [35] recorded the path of a camera, then a robot was used to play back this path and obtain 48 non-uniformly blurred images from four sharp images and 12 trajectories. Lai et al. [36] have released two datasets; one is a set of 100 real blurred images, and the other contains 200 synthetically blurred images that are both uniformly and non-uniformly blurred.

DOI: 10.54254/2755-2721/2026.GF36881

4.1.2. Real-world datasets

Synthetic datasets have good paired annotations, but the artificial blurring may not be the same as in real images. Rim et al. [33] introduced RealBlur, a real-world paired dataset, and also provided RealBlur-R, which is the raw camera image, and RealBlur-J, which is the camera-processed JPEG image. The set has 9,476 image pairs. Jiang et al. [37] employed a DAVIS240C camera to gather the Blur-DVS outdoor dataset. There are 1,782 training pairs, 396 test pairs, and also 740 real blurred images. Li et al. [25] have added ReLoBlur, a real-world local motion-deblurring dataset of compositing effects caused by locally moving objects and their backgrounds. ReLoBlur has 2010 training examples and 395 test examples.

4.2. Image quality assessment

Image-quality assessment methods are generally divided into subjective or objective. Subjective assessment relies on human perception. It usually does not depend on a reference image. One widely used metric is the mean opinion score (MOS) [38], which commonly rates visual quality on a five-point scale. Based on the availability of reference information, objective metrics are classified into three categories: full-reference, reduced-reference, and no-reference metrics.

4.2.1. Full-reference image quality

Assessment: Full-reference image quality assessment (FR-IQA) evaluates image restoration quality. The evaluation is performed by comparing the deblurred output with the ground-truth sharp image. Common metrics include peak signal-to-noise ratio (PSNR), structural similarity index measure (SSIM), multiscale structural similarity (MS-SSIM),and learned perceptual image patch similarity (LPIPS), among others. PSNR and SSIM are still widely used due to their simplicity and interpretability. In contrast, LPIPS often correlates more closely with human perceptual judgments.

4.2.2. Reduced-reference image quality assessment

Reduced-reference IQA (RR-IQA) compares statistical descriptors extracted from the restored and reference images without requiring exact pixel-wise correspondence. A representative metric is the Fréchet inception distance (FID), which measures the Fréchet distance between the means and covariances of feature distributions. A lower FID indicates greater distributional similarity. Although reduced-reference metrics combine some advantages of full-reference and no-reference evaluation, they may not fully reflect image fidelity and are used more frequently for assessing generative models.

4.2.3. No-reference image quality assessment

No-reference IQA (NR-IQA) evaluates image quality without access to a corresponding sharp reference. Representative methods include BIQI, BLINDS-II, BRISQUE, CORNIA, DIIVINE, NIQE, and SSEQ. In addition, task-oriented evaluation can indirectly assess deblurring performance by measuring its effect on downstream vision tasks, such as object detection and image recognition.

DOI: 10.54254/2755-2721/2026.GF36881

5. Conclusion

The three contents of this paper are as follows: First, it summarized the physical origin and mathematical model of the four types of blur, and discussed the limitations of the conventional method under spatially varying degradation. Second, there are four main deep architectures. CNNs are good at learning local features of images but cannot model global dependencies; RNNs can handle long-term dependencies in sequences, but they are slow to train due to sequential processing; GANs can generate realistic images, but it is difficult to train them reliably; Transformers are very good at capturing global context and are suitable for large-scale problems, but they have high computational requirements. Third, the survey lists some typical synthetic and real-world datasets and introduces all kinds of subjective, full-reference, reduced-reference and no-reference evaluation methods.

The next two will be as follows: First, in order to reduce the high resource consumption of the self-attention mechanism and keep the capacity for modelling the entire input, an efficient Transformer architecture and lightweight deployment should be employed in actual applications on mobile phones and embedded systems. Second, improved generalization to real-world blur and multimodal information should be investigated through domain adaptation, domain generalization, and unsupervised or semisupervised learning. Joint optimization of deblurring with high-level vision tasks, e.g., object detection and semantic segmentation, may further improve task relevance and robustness under complex degradations.

References

[1] Fergus, R., Singh, B., Hertzmann, A., Roweis, S. T., & Freeman, W. T. (2006). Removing camera shake from a single photograph. *ACM Transactions on Graphics, 25*(3), 787-794.

[2] Nah, S., Kim, T. H., & Lee, K. M. (2017). Deep multi-scale convolutional neural network for dynamic scene deblurring. *Proceedings of 2017 IEEE Conference on Computer Vision and Pattern Recognition*. Honolulu, USA, 257-265.

[3] Zhang, J. W., Pan, J. S., Ren, J., Song, Y. B., Bao, L. C., Lau, R. W. H., & Yang, M. H. (2018). Dynamic scene deblurring using spatially variant recurrent neural networks. *Proceedings of 2018 IEEE/CVF Conference on Computer Vision and Pattern Recognition*. Salt Lake City, USA, 2521-2529.

[4] Singh, D., & Sahu, M. R. (2013). A survey on various image deblurring techniques. *International Journal of Advanced Research in Computer and Communication Engineering, 116*, 15-18.

[5] Sun, J., Cao, W. F., Xu, Z. B., & Ponce, J. (2015). Learning a convolutional neural network for non-uniform motion blur removal. *Proceedings of 2015 IEEE Conference on Computer Vision and Pattern Recognition*. Boston, USA, 769-777.

[6] Son, C. H., & Park, H. M. (2011). A pair of noisy/blurry patches-based PSF estimation and channel-dependent deblurring. *IEEE Transactions on Image Processing, 57*(4), 1791-1799.

[7] Gong, D., Yang, J., Liu, L. Q., Zhang, Y. N., Reid, I., Shen, C. H., Van Den Hengel, A., & Shi, Q. F. (2017). From motion blur to motion flow: A deep learning solution for removing heterogeneous motion blur. *Proceedings of 2017 IEEE Conference on Computer Vision and Pattern Recognition (CVPR)*, 2319-2328. Honolulu, USA.

[8] Tao, X., Gao, H. Y., Shen, X. Y., Wang, J., & Jia, J. Y. (2018). Scale-recurrent network for deep image deblurring. *Proceedings of 2018 IEEE/CVF Conference on Computer Vision and Pattern Recognition*, 8174-8182. Salt Lake City, USA.

[9] Kupyn, O., Budzan, V., Mykhailych, M., Mishkin, D., & Matas, J. (2018). DeblurGAN: Blind motion deblurring using conditional adversarial networks. *Proceedings of 2018 IEEE/CVF Conference on Computer Vision and Pattern Recognition*, 8183-8192. Salt Lake City, USA.

[10] Kupyn, O., Martyniuk, T., Wu, J. R., & Wang, Z. Y. (2019). DeblurGAN-v2: Deblurring (orders-of-magnitude) faster and better. *Proceedings of 2019 IEEE/CVF International Conference on Computer Vision*, 8877-8886. Seoul, Korea(South).

[11] Dosovitskiy, A., Beyer, L., Kolesnikov, A., et al. (2020). An image is worth 16x16 words: Transformers for image recognition at scale. *arXiv preprint arXiv:2010.11929*.

DOI: 10.54254/2755-2721/2026.GF36881

[12] Choromanski, K., Likhosherstov, V., Dohan, D., et al. (2020). Rethinking attention with performers. *arXiv preprint arXiv:2009.14794*.
[13] Xu, X. Y., Pan, J. S., Zhang, Y. J., & Yang, M. H. (2018). Motion blur kernel estimation via deep learning. *IEEE Transactions on Image Processing, 27*(1), 194-205.
[14] Ren, D. W., Zhang, K., Wang, Q. L., Hu, Q. H., & Zuo, W. M. (2020). Neural blind deconvolution using deep priors. *Proceedings of 2020 IEEE/CVF Conference on Computer Vision and Pattern Recognition*. Seattle, USA, 3338-3347.
[15] Fang, Z. X., Wu, F. F., Dong, W. S., Li, X., Wu, J. J., & Shi, G. M. (2023). Self-supervised non-uniform kernel estimation with flow-based motion prior for blind image deblurring. *Proceedings of 2023 IEEE/CVF Conference on Computer Vision and Pattern Recognition*. Vancouver, Canada, 18105-18114.
[16] Dong, W. S., Wang, P. Y., Yin, W. T., Shi, G. M., Wu, F. F., & Lu, X. T. (2019). Denoising prior driven deep neural network for image restoration. *IEEE Transactions on Pattern Analysis and Machine Intelligence, 41*(10), 2305-2318.
[17] Zhang, K., Zuo, W. M., & Zhang, L. (2019). Deep plug-and-play super-resolution for arbitrary blur kernels. *Proceedings of 2019 IEEE/CVF Conference on Computer Vision and Pattern Recognition*. Long Beach, USA, 1671-1681.
[18] Cho, S. J., Ji, S. W., Hong, J. P., Jung, S. W., & Ko, S. J. (2021). Rethinking coarse-to-fine approach in single image deblurring. *Proceedings of 2021 IEEE/CVF International Conference on Computer Vision (ICCV)*. Montreal, Canada, 4621-4630.
[19] Gao, H. Y., Tao, X., Shen, X. Y., & Jia, J. Y. (2019). Dynamic scene deblurring with parameter selective sharing and nested skip connections. *Proceedings of 2019 IEEE/CVF Conference on Computer Vision and Pattern Recognition*. Long Beach, USA, 3843-3851.
[20] Park, D., Kang, D. U., Kim, J., & Chun, S. Y. (2020). Multi-temporal recurrent neural networks for progressive non-uniform single image deblurring with incremental temporal training. *Proceedings of the 16th European Conference on Computer Vision (ECCV)*. Glasgow, UK, 327-343.
[21] Zhang, L. M., Zhang, H. G., Chen, J. H., & Wang, L. (2020). Hybrid deblur net: Deep non-uniform deblurring with event camera. *IEEE Access, 8*, 148075-148083.
[22] Lu, B. Y., Chen, J. C., & Chellappa, R. (2020). UID-GAN: Unsupervised image deblurring via disentangled representations. *IEEE Transactions on Biometrics, Behavior, and Identity Science, 2*(1), 26-39.
[23] Zhang, K. H., Luo, W. H., Zhong, Y. R., Ma, L., Stenger, B., Liu, W., & Li, H. D. (2020). Deblurring by realistic blurring. *Proceedings of 2020 IEEE/CVF Conference on Computer Vision and Pattern Recognition (CVPR)*. Seattle, USA, 2734-2743.
[24] Yang, T., Ren, P. R., Xie, X. S., & Zhang, L. (2021). GAN prior embedded network for blind face restoration in the wild. *Proceedings of 2021 IEEE/CVF Conference on Computer Vision and Pattern Recognition*. Nashville, USA, 672-681.
[25] Li, H. Y., Zhang, Z. R., Jiang, T. T., Luo, P., Feng, H. J., & Xu, Z. H. (2023). Real-world deep local motion deblurring. *Proceedings of the 37th AAAI Conference on Artificial Intelligence*, 1314-1322. Washington, USA.
[26] LeCun, Y., Bottou, L., Bengio, Y., et al. (1998). Gradient-based learning applied to document recognition. *Proceedings of the IEEE, 86*(11), 2278-2324.
[27] Liu, Z., Lin, Y., Cao, Y., et al. (2021). Swin transformer: Hierarchical vision transformer using shifted windows. *arXiv preprint* arXiv:2103.14030.
[28] Hassani, A., Walton, S., Li, J., et al. (2022). Neighborhood attention transformer. *arXiv preprint* arXiv:2204.07143.
[29] Child, R., Gray, S., Radford, A., et al. (2019). Generating long sequences with sparse transformers. *arXiv preprint* arXiv:1904.10509.
[30] Wang, S., Li, B. Z., Khabsa, M., et al. (2020). Linformer: Self-attention with linear complexity. *arXiv preprint* arXiv:2004.04768.
[31] Katharopoulos, A., Vyas, A., Pappas, N., et al. (2020). Transformers are RNNs: Fast autoregressive transformers with linear attention. *Proceedings of the 37th International Conference on Machine Learning (ICML)*. Online, 5156-5165.
[32] Levin, A., Weiss, Y., Durand, F., & Freeman, W. T. (2009). Understanding and evaluating blind deconvolution algorithms. *Proceedings of 2009 IEEE Conference on Computer Vision and Pattern Recognition*. Miami, USA, 1964-1971.
[33] Rim, J., Lee, H., Won, J., & Cho, S. (2020). Real-world blur dataset for learning and benchmarking deblurring algorithms. *Proceedings of the 16th European Conference on Computer Vision (ECCV)*. Glasgow, UK, 184-201.
[34] Sun, L. B., Cho, S., Wang, J., & Hays, J. (2013). Edge-based blur kernel estimation using patch priors. *Proceedings of 2013 IEEE International Conference on Computational Photography (ICCP)*. Cambridge, USA, 1-8.

DOI: 10.54254/2755-2721/2026.GF36881

[35] Köhler, R., Hirsch, M., Mohler, B., Schölkopf, B., & Harmeling, S. (2012). Recording and playback of camera shake: Benchmarking blind deconvolution with a real-world database. *Proceedings of the 12th European Conference on Computer Vision (ECCV)*. Florence, Italy, 27-40.

[36] Lai, W. S., Huang, J. B., Hu, Z., Ahuja, N., & Yang, M. H. (2016). A comparative study for single image blind deblurring. *Proceedings of 2016 IEEE Conference on Computer Vision and Pattern Recognition*. Las Vegas, USA, 1701-1709.

[37] Jiang, Z., Zhang, Y., Zou, D. Q., Ren, J., Lv, J. C., & Liu, Y. B. (2020). Learning event-based motion deblurring. *Proceedings of 2020 IEEE/CVF Conference on Computer Vision and Pattern Recognition*, 3317–3326. Seattle, USA.

[38] Hossfeld, T., Heegaard, P. E., Varela, M., et al. (2016). QoE beyond the MOS: An in-depth look at QoE via better metrics and their relation to MOS. *Quality and User Experience, 1*(1), 2.